

The cytokine receptor DR3 identifies and activates thymic NKT17 cells

Shunqun Luo^{1,2}, Nurcin Liman^{1,2}, Assiatu Crossman¹, and Jung-Hyun Park^{1,*}

¹Experimental Immunology Branch, Center for Cancer Research, National Cancer Institute, NIH, Bethesda, MD 20892; ²contributed equally

Running title: DR3 is a functional marker of thymic NKT17 cells

***Address to correspondence to:**

Jung-Hyun Park
Experimental Immunology Branch
Center for Cancer Research, NCI, NIH
Building 10, Room 5B17
10 Center Dr., Bethesda, MD 20892
E-mail: Parkhy@mail.nih.gov

28 **Abstract**

29 Invariant natural killer T (*i*NKT) cells are thymus-generated T cells with innate-like
30 characteristics and effector function. Several functionally distinct *i*NKT subsets have been
31 identified, but NKT17 is the only *i*NKT subset that produces the proinflammatory cytokine
32 IL-17. NKT17 cells are generated in the thymus and then exported into the periphery to
33 populate lymphoid organs and barrier tissues, such as the lung, to provide critical support in
34 host defense. However, the molecular mechanisms that drive the thymic development and
35 subset-specific activation of NKT17 cells remain mostly unknown. Here, we identify the
36 cytokine receptor DR3, a member of the TNF receptor superfamily, being selectively
37 expressed on NKT17 cells but absent on all other thymic *i*NKT subsets. We further
38 demonstrate that DR3 ligation leads to the *in vivo* activation of thymic NKT17 cells and
39 provides *in vitro* costimulatory effects upon α -GalCer-stimulation. Thus, our study reports
40 the identification of a specific surface marker for thymic NKT17 cells that selectively
41 triggers their activation both *in vivo* and *in vitro*. These findings provide new insights for
42 deciphering the role and function of IL-17-producing NKT17 cells and for understanding the
43 development and activation mechanisms of *i*NKT cells in general.

44

45 **Keywords:** CD138, IL-17, *i*NKT cells, ROR γ t, thymus.

46

47 **Introduction**

48 *i*NKT cells are thymus-derived effector T cells expressing a semi-invariant V α 14-J α 18 T cell
49 receptor (TCR) that equips them with the ability to recognize microbial glycolipids in the context
50 of the nonclassical MHC-I molecule CD1d. Unlike conventional $\alpha\beta$ T cells, *i*NKT cells possess
51 the innate ability to express effector molecules and proinflammatory cytokines prior to their
52 exposure to antigens. While *i*NKT cells are few in their number and limited in their TCR
53 repertoire, *i*NKT cells play critical roles in immunosurveillance, inflammation, and host defense
54 (*Bendelac et al., 2007; Crosby et al., 2018*). There are several subsets of *i*NKT cells, among
55 which three major populations, *i.e.*, NKT1, NKT2, and NKT17, have been identified (*Lee et al.,*
56 *2013*). In particular, NKT17 cells are noted for their ability to produce the proinflammatory
57 cytokine IL-17 and to express the transcription factor ROR γ t (*Lee et al., 2013*). NKT17 cells can
58 be identified by their distinct expression of the cell surface marker CD138 (Syndecan-1) (*Dai et*
59 *al., 2015*). However, the role of CD138 in NKT17 cell biology remains mostly unclear (*Dai et*
60 *al., 2015*)[Please add: Luo S., 2021, JCI Insight]. Because NKT17 cells are the major producers
61 of IL-17 in the thymus and in barrier tissues, such as the lung and skin (*Tsagaratou, 2019*), there
62 is a keen interest in delineating the developmental requirements and activation mechanism of
63 NKT17 cells. Here, we report the surprising finding that the TNF receptor superfamily member
64 Death Receptor-3 (DR3) is highly and specifically expressed on thymic NKT17 cells, and that
65 the stimulation of DR3 using agonistic anti-DR3 antibodies leads to the activation of NKT17
66 cells in the thymus, unveiling a new layer of control in NKT17 cell biology.

67

68

69 **Results and Discussion**

70 *The cytokine receptor DR3 is specifically expressed on thymic NKT17 cells*

71 We embarked on this study to uncover new regulatory mechanisms and effector functions that
72 are specifically associated with individual *i*NKT subsets, and particularly with NKT17 cells.
73 While CD138 is a specific marker for NKT17 cells, CD138 is not required for their generation or
74 effector function (*Dai et al., 2015; Luo et al., 2021*) Thus, functional markers for NKT17 cells
75 are currently not available. Because cytokines play critical roles in the generation and survival of
76 *i*NKT cells (*Bendelac et al., 2007; Crosby et al., 2018*), we screened a panel of cytokine
77 receptors for their *i*NKT subset-specific expression, and here we identified the TNF receptor
78 superfamily member 25 (TNFRS25), also known as DR3 (*Meylan et al., 2011*), being highly
79 expressed on thymic NKT17 cells (**Figure 1A and 1B**). As expected, DR3 expression correlated
80 closely with CD138 expression in thymic *i*NKT cells of both C57BL/6 and BALB/c mice
81 (**Figure 1A, 1B; Figure 1–figure supplement 1**). On the other hand, DR3 expression was
82 independent of CD138 because DR3 was still abundantly and specifically found on NKT17 cells
83 of CD138-deficient (*Sdc1^{-/-}*) BALB/c mice (**Fig. 1C**). Furthermore, the forced expression of
84 ROR γ t (*Ligons et al., 2018*), the master transcription factor of NKT17 cell development and
85 function (*Tsagaratou, 2019*), dramatically increased both the frequency and number of DR3-
86 expressing *i*NKT cells (**Figure 1D**). These results suggested that DR3 expression is controlled
87 downstream of ROR γ t so that all DR3⁺ thymic *i*NKT cells of ROR γ t^{Tg} mice also expressed
88 CD138 (**Figure 1D; Figure 1–figure supplement 2**).

89 DR3 is the receptor for the cytokine TNF-like ligand 1A (TL1A) (*Valatas et al., 2019*).
90 Consistent with the notion that DR3 is highly expressed on Foxp3⁺ Treg cells (*Nishikii et al.,*
91 *2016*), the stimulation with TL1A or the ligation of DR3 with agonistic anti-DR3 antibodies

92 triggers the activation of Foxp3⁺ Treg cells (*Nishikii et al., 2016*). Because we found NKT17
93 cells to express DR3, we thus asked whether DR3 ligation would also activate thymic NKT17
94 cells. To this end, we injected BALB/c mice with agonistic anti-DR3 antibodies and assessed
95 their effect on thymic *i*NKT cells. Of note, we utilized BALB/c mice that were engineered to
96 express *Foxp3*-GFP reporter proteins (Foxp3-DTR/EGFP mice) (*Kim et al., 2007*), which
97 allowed us to verify the *in vivo* effect of anti-DR3 injection. Indeed, assessing GFP-expressing
98 CD4 T cells confirmed that DR3 ligation induced the expansion of Foxp3⁺ Treg cells (**Figure**
99 **2A**). Curiously, while both the frequency and number of Foxp3⁺ cells were significantly
100 increased in DR3-injected mice, at the same time, the frequency and number of thymic NKT17
101 cells were dramatically diminished (**Figure 2B**). Thus, DR3 ligation clearly affected NKT17
102 cells, but DR3 activation appeared to be detrimental instead of stimulatory for thymic NKT17
103 cells.

104 Because we identified NKT17 cells based on their CD138 expression (*Luo et al., 2021*),
105 we could not exclude the possibility that DR3 ligation would appear to deplete NKT17 cells by
106 downregulating CD138 expression. In fact, the shedding of the CD138 ectodomain is a well-
107 described process that results in the loss of surface CD138 (*Rangarajan et al., 2020*), so that
108 DR3 ligation might have triggered CD138 downregulation without altering the composition of
109 the thymic *i*NKT cells. To determine whether DR3 ligation leads to the actual loss of NKT17
110 cells or if anti-DR3 only induces the downregulation of surface CD138 expression on NKT17
111 cells, we considered it necessary to identify NKT17 cells with markers other than surface
112 CD138. Hence, we employed the surface markers CD4 and CD122 to discriminate individual
113 *i*NKT subsets (*Georgiev et al., 2016*). CD122 is selectively expressed on NKT1 cells (*Won et al.,*
114 *2021*), so that CD122⁺ *i*NKT cells correspond to the NKT1 subset. NKT2 cells are CD122-

115 negative but they express large amounts of CD4 (CD122⁻CD4⁺). Most NKT17 cells, on the other
116 hand, are negative for both CD4 and CD122 (*Georgiev et al., 2016*). In fact, CD122/CD4
117 double-negative (DN) cells were ROR γ t⁺ and expressed high levels of both DR3 and CD138,
118 confirming that they corresponded to NKT17 cells (**Figure 3A**). Therefore, the combined use of
119 CD122 and CD4 permitted us to identify NKT17 subset cells without using CD138. In
120 agreement, DR3 was also highly expressed on the DN *i*NKT cells of CD138-deficient *Sdc1*^{-/-}
121 mice, marking them as NKT17 cells, (**Figure 3B**). These results indicated that DR3 expression is
122 a bona fide marker for thymic NKT17 cells, independently of CD138.

123

124 ***DR3 ligation selectively activates thymic NKT17 cells***

125 Equipped with this toolkit to identify NKT17 cells, we next assessed the effect of DR3 ligation
126 on NKT17 cells. Injection of agonistic anti-DR3 antibodies into BALB/c mice induced the
127 expression of CD69, a classical activation marker (*Ziegler et al., 1994*), on thymic NKT17 cells
128 which was accompanied by decreased CD138 expression (**Figure 3C**). Consequently, the loss of
129 CD138⁺ *i*NKT cells upon DR3 injection (**Figure 2B**) is unlikely due to the loss of NKT17 cells
130 but more likely the result of their selective activation. Indeed, DR3-induced activation was
131 largely limited to thymic NKT17 cells with minimal or no activation of NKT1 and NKT2 cells
132 (**Figure 3C; Figure 3–figure supplement 1**). Importantly, DR3 signaling was reported to
133 require the co-expression of galectin-9 (*Madireddi et al., 2017*), and we found that NKT17 cells
134 were incidentally the only thymic *i*NKT subset that expressed both DR3 and galectin-9 (**Figure**
135 **3D; Figure 3–figure supplement 2**).

136 While the injection of anti-DR3 antibodies activated NKT17 cells *in vivo*, anti-DR3
137 antibodies alone were insufficient to induce their activation *in vitro* (**Figure 3E**). However, DR3

138 ligation significantly boosted the effect of α -GalCer stimulation and bolstered the expression of
139 the activation markers CD25 and CD69 on NKT17 cells (**Figure 3E; Figure 3–figure**
140 **supplement 3**), indicating that DR3 acts as a costimulatory molecule. Altogether, these results
141 suggested that DR3 is a functional marker for NKT17 cells through which the *i*NKT immune
142 response can be skewed towards IL-17 immunity. Finally, we examined whether CD138 is a
143 prerequisite for DR3-induced activation of CD138 for NKT17 cells (*Dai et al., 2015*). Here, we
144 found that *Sdc1*^{-/-} NKT17 cells still responded robustly to DR3 ligation so that the activation-
145 induced upregulation of CD69 was comparable to that of WT NKT17 cells (**Figure 3F**).
146 Therefore, CD138 is specifically expressed on NKT17 cells but not required for DR3-induced
147 NKT17 activation.

148 Collectively, our results identified the cytokine receptor DR3 as a new costimulatory
149 molecule that is specifically expressed on and activates thymic NKT17 cells. In this regard, DR3
150 represents a new class of immunomodulatory molecules whose expression and function are
151 linked to a specific *i*NKT subset. These results open new avenues for elucidating how different
152 *i*NKT subsets, that express the same invariant TCR and respond to the same agonistic glycolipid,
153 *i.e.*, α -GalCer, can elicit subset-specific immune responses *in vivo*.

154

155 **Materials and Methods**

156

157 ***Mice***

158 BALB/cAnNCr1 and C57BL/6 mice were purchased from the Charles River Laboratories.

159 CD138-deficient (*Sdc1*^{-/-}) mice and ROR γ ^{Tg} mice were previously described (*Alexander et al.,*
160 *2000; Ligons et al., 2018; Luo et al., 2021*), and these animals were backcrossed in-house onto

161 BALB/cAnNCrl background before analyses. Foxp3-DTR/EGFP mice were obtained from the
162 Jackson Laboratory and maintained on BALB/cAnNCrl background (*Lahl et al., 2007*). Animal
163 experiments were approved by the NCI Animal Care and Use Committee. All mice were cared
164 for in accordance with the NIH guidelines.

165

166 ***Antibodies***

167 Antibodies specific for the following antigens were used for staining: TCR β (H57-597), CD4
168 (GK1.5), CD24 (M1/69), CD138 (181-2), CD122 (TM- β 1), CD44 (IM7), DR3 (4C12), Galectin-
169 9 (108A2), CD69 (H1.2F3), CD25 (PC61.5), IL-7R α (A7R34), IL-17 (eBio17B7), PLZF (9E12),
170 and ROR γ t (Q31-378). Armenian Hamster IgG isotype Control Antibody (HTK888) was used as
171 control for anti-DR3 staining. Rat IgG2a, κ Isotype Ctrl (RTK2758) was used as control for anti-
172 Galectin-9 staining. PBS-57-loaded mouse CD1d tetramers were obtained from NIH Tetramer
173 Core Facility (Emory University, Atlanta, GA).

174

175 ***Enrichment of mature thymocytes***

176 CD24-negative mature thymocytes were enriched by magnetic depletion of CD24⁺ cells, as
177 previously described (*Park, Kwon, et al., 2019*). In brief, total thymocytes were processed to
178 single cell suspension in 10% FBS/HBSS (20×10^6 cells/ml) and incubated with rat anti-mouse
179 CD24 antibodies (M1/69, Biolegend) ($30 \mu\text{g}/100 \times 10^6$ cells) for 30 mins on ice. After washing
180 off excess reagents, thymocytes were mixed with anti-rat IgG-conjugated BioMag beads
181 (QIAGEN) and incubated for 45 mins at 4°C on a MACSmix Tube Rotator (Miltenyi Biotec).
182 Anti-CD24 antibody-bound cells were then magnetically removed, and non-binding cells were
183 harvested for further experiments.

184

185 ***Flow cytometry***

186 Fluorescence antibody-stained single-cell suspensions were analyzed using LSRFortessa or
187 LSRII flow cytometers (BD Biosciences). For live cell analysis, dead cells were excluded by
188 adding propidium iodide before running the samples on flow cytometers. For fixed cell staining
189 and analysis, cells were stained with Ghost Dye Violet 510 (Tonbo) for exclusion of dead cells,
190 followed by surface staining and fixation with Foxp3 fixation buffer (eBioscience). Afterwards,
191 cells were permeabilized using reagents from the Foxp3 intracellular kit according to the
192 manufacturer's instructions (eBioscience). Excess reagents were removed by extensive washing
193 in FACS buffer (0.5% BSA, 0.1% sodium azide in HBSS) before analysis.

194

195 ***Identification of iNKT subsets by intracellular staining***

196 Thymic iNKT subsets were identified by staining for transcription factors as previously
197 described (*Park, DiPalma, et al., 2019*). In brief, thymocytes were stained with fluorescence-
198 conjugated PBS-57-loaded mouse CD1d tetramers, followed by antibody staining for other
199 surface markers for 40 minutes. After washing out excess reagents, cells were fixed in 150 µl of
200 a 1:3 mixture of concentrate/diluent working solution of the Foxp3 Fixation Buffer and further
201 diluted with 100 µl FACS buffer. After 20 minutes at room temperature, cells were washed twice
202 with permeabilization buffer (eBioscience) before adding antibodies for transcription factor
203 staining. After 1 hour of incubation at room temperature, cells were washed, resuspended in
204 FACS buffer, and analyzed by flow cytometry.

205

206 ***Anti-DR3 agonistic antibody injection***

207 For *in vivo* anti-DR3 ligation, mice were injected i.p. with either 10 µg anti-DR3 antibody
208 (4C12, Biolegend) or 10 µg Armenian Hamster IgG control antibody (HTK888, Biolegend). One
209 week after injection, thymus and spleen were harvested for further analysis.

210

211 ***In vitro* stimulation of thymic iNKT cells**

212 Single cell suspension of freshly isolated thymocytes were plated into 24-well plates at 2×10^6
213 cells/mL with 100 ng/mL of α -GalCer in the presence or absence of anti-DR3 antibody (2
214 µg/mL) or with anti-DR3 antibody alone (10 µg/mL) (*Schreiber et al., 2010*). Cells were
215 cultured overnight at 37°C in a 7.5% CO₂ incubator before analysis by flow cytometry.

216

217 ***Statistics***

218 Data are shown as the mean \pm SEM. Two-tailed Student's *t*-test was used to calculate P values. P
219 values of less than 0.05 were considered significant, where NS indicates not significant.

220 Statistical data were analyzed using the GraphPad Prism 8 software.

221

222 **Acknowledgement**

223 This study was supported by the Intramural Research Program of the US National Institutes of
224 Health, National Cancer Institute, Center for Cancer Research.

225

226 **Authorship Contribution:** SL and NL designed and performed the experiments, analyzed the
227 data, and contributed to the writing of the manuscript. AC performed experiments, analyzed the
228 data, and commented on the manuscript. JP conceived the project, analyzed the data, and wrote
229 the manuscript.

230

231 **Conflict-of-interest disclosure:** The authors declare no competing financial interests.

232

233 **ORCID profiles:** S.L., 0000-0002-5728-2112; N.L.,0000-0002-2910-1070; A.C.,0000-0001-

234 5746-0073; J.H.P., 0000-0002-9547-9055.

235 **References**

- 236
- 237 Alexander CM, Reichsman F, Hinkes MT, Lincecum J, Becker KA, Cumberledge S, Bernfield
238 M. (2000). Syndecan-1 is required for Wnt-1-induced mammary tumorigenesis in mice.
239 *Nat Genet*, 25(3), 329-332. <https://doi.org/10.1038/77108>
- 240
- 241 Bendelac A, Savage PB, Teyton L. (2007). The biology of NKT cells. *Annu Rev Immunol*, 25,
242 297-336. <https://doi.org/10.1146/annurev.immunol.25.022106.141711>
- 243 Crosby CM, Kronenberg M. (2018). Tissue-specific functions of invariant natural killer T cells.
244 *Nat Rev Immunol*, 18(9), 559-574. <https://doi.org/10.1038/s41577-018-0034-2>
- 245
- 246 Dai H, Rahman A, Saxena A, Jaiswal AK, Mohamood A, Ramirez L, Noel S, Rabb H, Jie C,
247 Hamad AR. (2015). Syndecan-1 identifies and controls the frequency of IL-17-producing
248 naive natural killer T (NKT17) cells in mice. *Eur J Immunol*, 45(11), 3045-3051.
249 <https://doi.org/10.1002/eji.201545532>
- 250
- 251 Georgiev H, Ravens I, Benarafa C, Forster R, Bernhardt G. (2016). Distinct gene expression
252 patterns correlate with developmental and functional traits of iNKT subsets. *Nat*
253 *Commun*, 7, 13116. <https://doi.org/10.1038/ncomms13116>
- 254
- 255 Kim JM, Rasmussen JP, Rudensky AY. (2007). Regulatory T cells prevent catastrophic
256 autoimmunity throughout the lifespan of mice. *Nat Immunol*, 8(2), 191-197.
257 <https://doi.org/10.1038/ni1428>
- 258
- 259 Lahl K, Loddenkemper C, Drouin C, Freyer J, Arnason J, Eberl G, Hamann A, Wagner H,
260 Huehn J, Sparwasser T. (2007). Selective depletion of Foxp3+ regulatory T cells induces
261 a scurfy-like disease. *J Exp Med*, 204(1), 57-63. <https://doi.org/10.1084/jem.20061852>
- 262
- 263 Lee YJ, Holzapfel KL, Zhu J, Jameson SC, Hogquist KA. (2013). Steady-state production of IL-
264 4 modulates immunity in mouse strains and is determined by lineage diversity of iNKT
265 cells. *Nat Immunol*, 14(11), 1146-1154. <https://doi.org/10.1038/ni.2731>
- 266
- 267 Ligons DL, Hwang S, Waickman AT, Park JY, Luckey MA, Park JH. (2018). RORgammat
268 limits the amount of the cytokine receptor gammac through the prosurvival factor Bcl-xL
269 in developing thymocytes. *Sci Signal*, 11(545). <https://doi.org/10.1126/scisignal.aam8939>
- 270
- 271 Luo S, Kwon J, Crossman A, Park PW, Park JH. (2021). CD138 expression is a molecular
272 signature but not a developmental requirement for RORgammat+ NKT17 cells. *JCI*
273 *Insight*, 6(18). <https://doi.org/10.1172/jci.insight.148038>
- 274
- 275 Madireddi S, Eun SY, Mehta AK, Birta A, Zajonc DM, Niki T, Hirashima M, Podack ER,
276 Schreiber TH, Croft M. (2017). Regulatory T Cell-Mediated Suppression of
277 Inflammation Induced by DR3 Signaling Is Dependent on Galectin-9. *J Immunol*, 199(8),
278 2721-2728. <https://doi.org/10.4049/jimmunol.1700575>
- 279

- 280 Meylan F, Richard AC, Siegel RM. (2011). TL1A and DR3, a TNF family ligand-receptor pair
281 that promotes lymphocyte costimulation, mucosal hyperplasia, and autoimmune
282 inflammation. *Immunol Rev*, 244(1), 188-196. [https://doi.org/10.1111/j.1600-](https://doi.org/10.1111/j.1600-065X.2011.01068.x)
283 [065X.2011.01068.x](https://doi.org/10.1111/j.1600-065X.2011.01068.x)
284
- 285 Nishikii H, Kim BS, Yokoyama Y, Chen Y, Baker J, Pierini A, Alvarez M, Mavers M, Maas-
286 Bauer K, Pan Y, Chiba S, Negrin RS. (2016). DR3 signaling modulates the function of
287 Foxp3+ regulatory T cells and the severity of acute graft-versus-host disease. *Blood*,
288 128(24), 2846-2858. <https://doi.org/10.1182/blood-2016-06-723783>
289
- 290 Park JY, DiPalma DT, Kwon J, Fink J, Park JH. (2019). Quantitative Difference in PLZF Protein
291 Expression Determines iNKT Lineage Fate and Controls Innate CD8 T Cell Generation.
292 *Cell Rep*, 27(9), 2548-2557 e2544. <https://doi.org/10.1016/j.celrep.2019.05.012>
293
- 294 Park JY, Kwon J, Kim EY, Fink J, Kim HK, Park JH. (2019). CD24(+) Cell Depletion Permits
295 Effective Enrichment of Thymic iNKT Cells While Preserving Their Subset
296 Composition. *Immune Netw*, 19(2), e14. <https://doi.org/10.4110/in.2019.19.e14>
297
- 298 Rangarajan S, Richter JR, Richter RP, Bandari SK, Tripathi K, Vlodaysky I, Sanderson RD.
299 (2020). Heparanase-enhanced Shedding of Syndecan-1 and Its Role in Driving Disease
300 Pathogenesis and Progression. *J Histochem Cytochem*, 68(12), 823-840.
301 <https://doi.org/10.1369/0022155420937087>
302
- 303 Schreiber TH, Wolf D, Tsai MS, Chirinos J, Deyev VV, Gonzalez L, Malek TR, Levy RB,
304 Podack ER. (2010). Therapeutic Treg expansion in mice by TNFRSF25 prevents allergic
305 lung inflammation. *J Clin Invest*, 120(10), 3629-3640. <https://doi.org/10.1172/JCI42933>
306
- 307 Tsagaratou A. (2019). Unveiling the regulation of NKT17 cell differentiation and function. *Mol*
308 *Immunol*, 105, 55-61. <https://doi.org/10.1016/j.molimm.2018.11.013>
309
- 310 Valatas V, Kolios G, Bamias G. (2019). TL1A (TNFSF15) and DR3 (TNFRSF25): A Co-
311 stimulatory System of Cytokines With Diverse Functions in Gut Mucosal Immunity.
312 *Front Immunol*, 10, 583. <https://doi.org/10.3389/fimmu.2019.00583>
313
- 314 Won HY, Kim HK, Crossman A, Awasthi P, Gress RE, Park JH. (2021). The Timing and
315 Abundance of IL-2Rbeta (CD122) Expression Control Thymic iNKT Cell Generation
316 and NKT1 Subset Differentiation. *Front Immunol*, 12, 642856.
317 <https://doi.org/10.3389/fimmu.2021.642856>
318
- 319 Ziegler SF, Ramsdell F, Alderson MR. (1994). The activation antigen CD69. *Stem Cells*, 12(5),
320 456-465. <https://doi.org/10.1002/stem.5530120502>

321
322

323 **Figure legend**

324 **Figure 1. DR3 is specifically expressed on thymic NKT17 cells**

325 **A.** *i*NKT subsets were identified among the thymocytes of BALB/c mice by staining for the
326 intracellular proteins ROR γ t and PLZF and measuring the subset-specific expression of DR3 and
327 CD138. The data are representative of 2 independent experiments with a total 4 BALB/c mice.

328 **B.** Quantification of DR3 and CD138 expression (Δ MFI) in individual *i*NKT subsets. The data
329 show the summary of 2 independent experiments with a total of at least 4 BALB/c mice.
330 Statistical significance was determined by unpaired two-tailed Student's *t*-tests.

331 **C.** DR3 and CD138 expression on thymic NKT17 cells of CD138-deficient (*Sdc1*^{-/-}) and
332 littermate control (WT) BALB/c mice. The data are representative of 2 independent experiments
333 with a total 4 *Sdc1*^{-/-} and 4 WT BALB/c mice.

334 **D.** Thymic *i*NKT cells of ROR γ t^{Tg} and littermate control (WT) BALB/c thymocytes were
335 assessed for surface DR3 and CD138 expression. The contour plot is representative (left), and
336 the bar graphs (right) are a summary of data from three independent experiments with a total of 6
337 ROR γ t^{Tg} and 6 WT mice. Statistical significance was determined by paired two-tailed Student's
338 *t*-tests.

339 The following figure supplements are available for Figure 1:

340 **Figure supplement 1.** DR3 expression on thymic NKT17 cells of C57BL/6 mice.

341 **Figure supplement 2.** Thymic CD138⁺ *i*NKT cells in WT and ROR γ t^{Tg} BALB/c mice.

342

343 **Figure 2. *In vivo* effects of DR3 ligation on Foxp3⁺ Treg and CD138⁺ NKT17 cells**

344 **A.** Contour plots show *Foxp3*-GFP versus CD25 expression of spleen CD4⁺ T cells (left), and
345 bar graphs show the frequencies and cell numbers of splenic CD25⁺Foxp3⁺ Treg cells (right),

346 after 1 week of injection with anti-DR3 or isotype control antibodies into BALB/c *Foxp3*-GFP
347 reporter mice. The results are summarized from 4 independent experiments with a total of 4 mice
348 injected with anti-DR3 and 4 mice injected with isotype control. Statistical significance was
349 determined by paired two-tailed Student's *t*-tests.

350 **B.** Identification and enumeration of CD138⁺ thymic *i*NKT cells among BALB/c *Foxp3*-GFP
351 reporter mice one week after injection of anti-DR3 or isotype control antibody (Ctrl IgG). The
352 contour plot is representative, and the bar graphs are a summary of data from 11 independent
353 experiments with a total of 11 mice for each group. Statistical significance was determined by
354 paired two-tailed Student's *t*-tests.

355

356 **Figure 3. DR3 is a specific and functional marker of thymic NKT17 cells**

357 **A.** Thymic *i*NKT subsets were identified by CD4 versus CD122 expression (contour plot), and
358 the expression of subset-specific signature molecules were quantified for the indicated *i*NKT
359 subsets (bar graphs). The contour plot is representative, and the bar graphs are summaries of data
360 from three independent experiments with a total of 3 BALB/c mice. Statistical significance was
361 determined by unpaired two-tailed Student's *t*-tests.

362 **B.** DR3 expression on CD4, CD122-disparate thymic *i*NKT subsets of CD138-deficient (*Sdc1*^{-/-})
363 BALB/c mice. The bar graph shows the summary of data from three independent experiments
364 with a total of 5 *Sdc1*^{-/-} BALB/c mice. Statistical significance was determined by unpaired two-
365 tailed Student's *t*-tests.

366 **C.** Activation marker expression on thymic NKT17 cells of BALB/c *Foxp3*-GFP reporter mice
367 upon anti-DR3 antibody injection. The contour plot is representative, and the bar graphs are
368 summaries of data from 7 independent experiments with a total of 14 BALB/c *Foxp3*-GFP

369 reporter mice injected either with anti-DR3 (7 mice) or isotype control antibodies (7 mice).

370 Statistical significance was determined by paired two-tailed Student's *t*-tests.

371 **D.** DR3 and Galectin-9 co-expression on thymic *i*NKT subsets of BALB/c mice identified by the
372 CD4 versus CD122 expression. The graph is a summary of data from 2 independent experiments
373 with a total of 5 BALB/c mice.

374 **E.** *In vitro* activation of thymic NKT17 cells by overnight stimulation with α -GalCer (100 ng/ml)
375 in the presence or absence of anti-DR3 antibody (2 μ g/ml) stimulation. The bar graph is a
376 summary of data from 4 independent experiments with a total of 10 BALB/c mice. Statistical
377 significance was determined by paired two-tailed Student's *t*-tests.

378 **F.** CD69 expression on thymic NKT17 cells from *Sdc1*^{-/-} and littermate control (WT) BALB/c
379 mice one week after injection with anti-DR3 or isotype control antibodies (Ctrl IgG). The bar
380 graph is a summary of data from 4 independent experiments with a total of 4 mice for each
381 group. Statistical significance was determined by unpaired two-tailed Student's *t*-tests.

382 The following figure supplements are available for Figure 3:

383 **Figure supplement 1.** CD69 expression upon DR3 injection in thymic NKT1 and NKT2 cells.

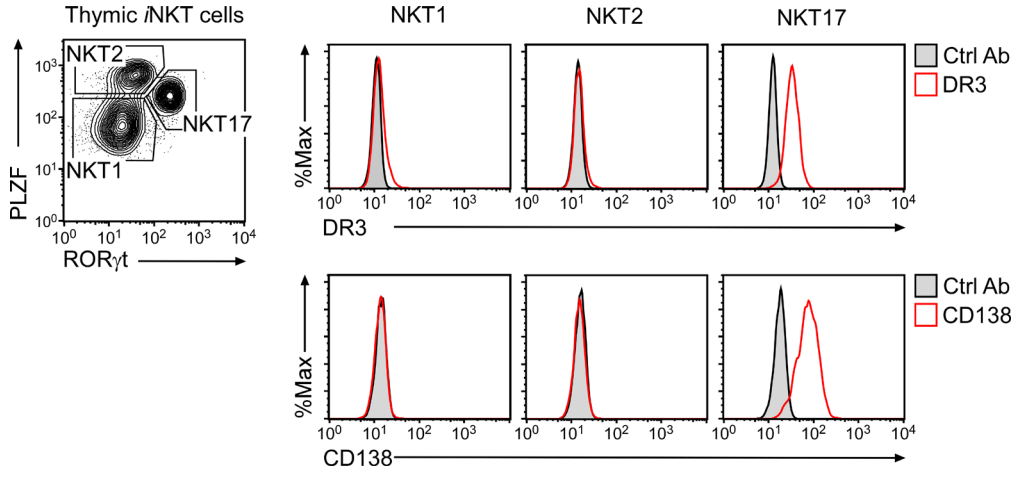
384 **Figure supplement 2.** Galectin-9 and DR3 expression in thymic *i*NKT cell subsets of BALB/c
385 mice.

386 **Figure supplement 3.** *In vitro* stimulation of thymic *i*NKT cells with α -GalCer and/or anti-DR3
387 antibodies.

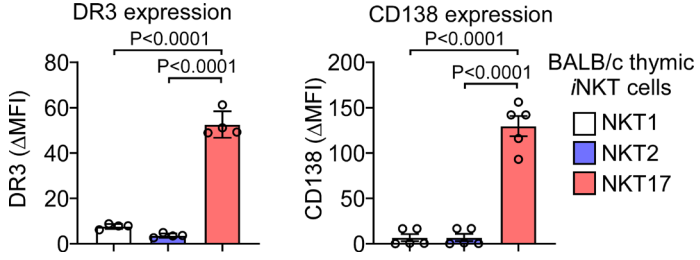
388

Figure 1

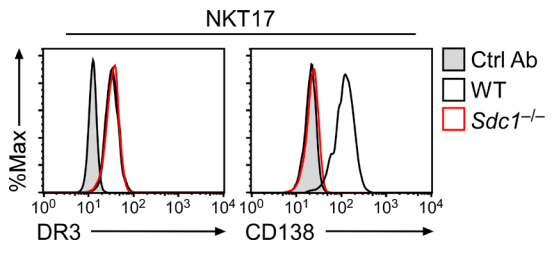
A



B



C



D

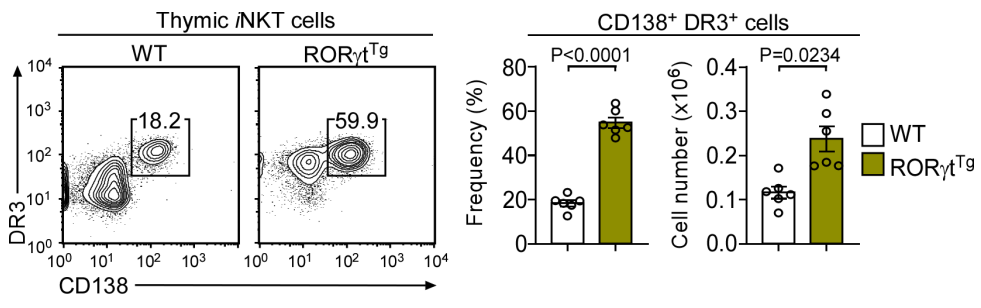
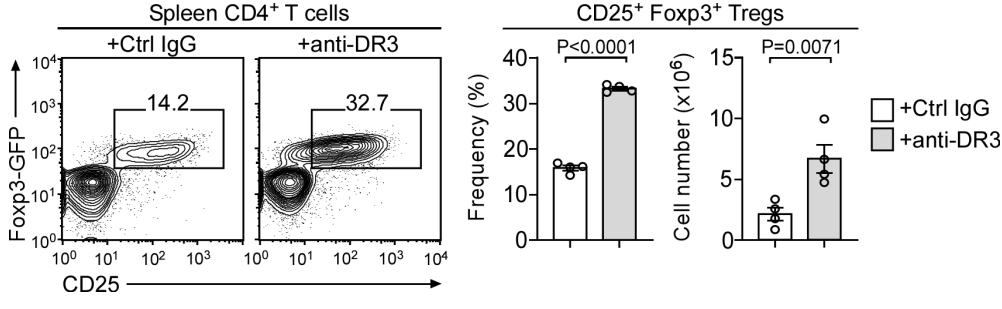


Figure 2

A



B

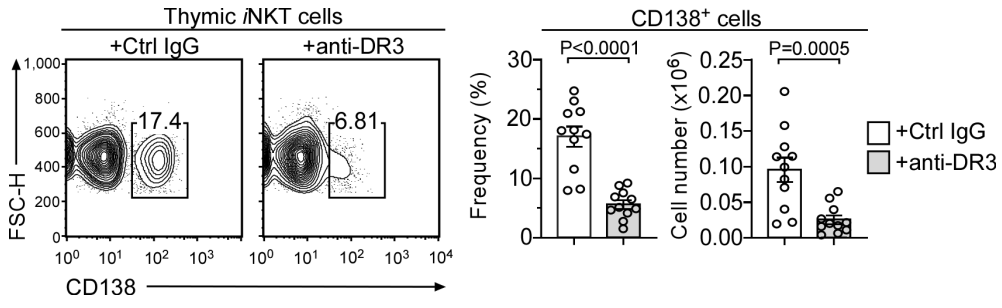


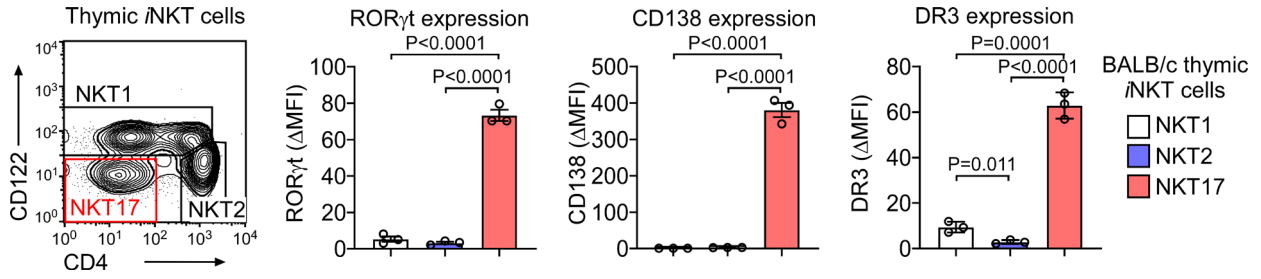
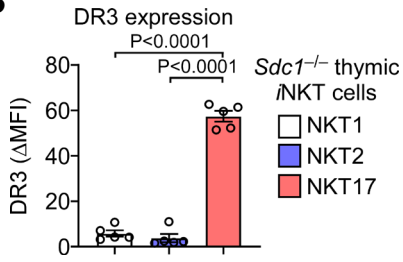
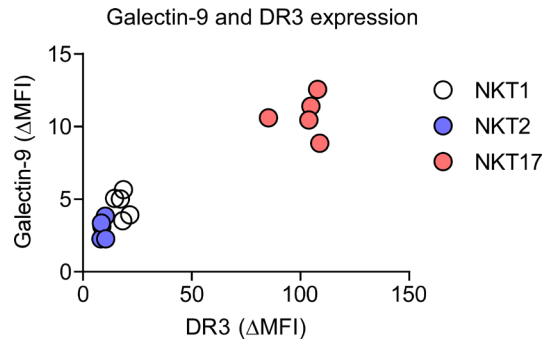
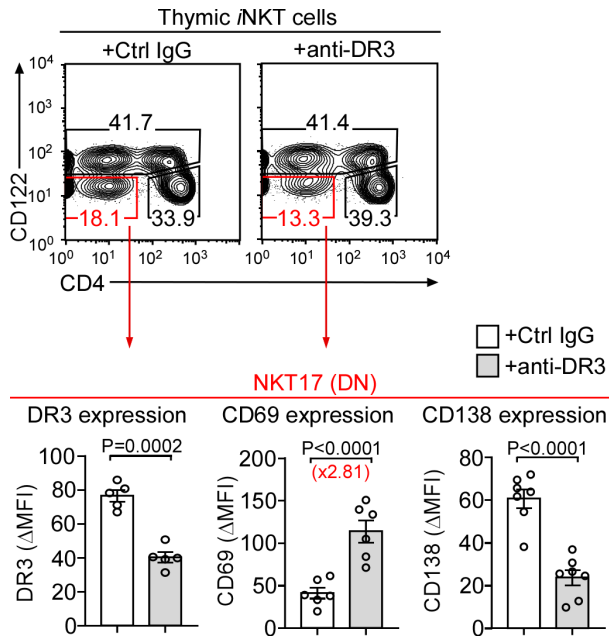
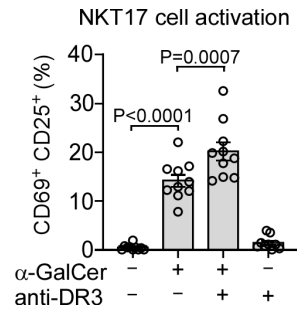
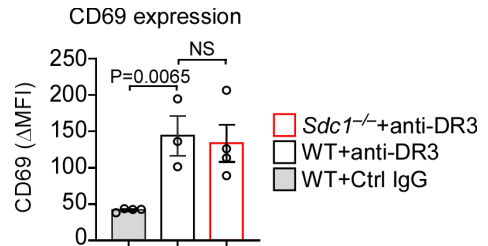
Figure 3**A****B****D****C****E****F**

Figure 1–figure supplement 1

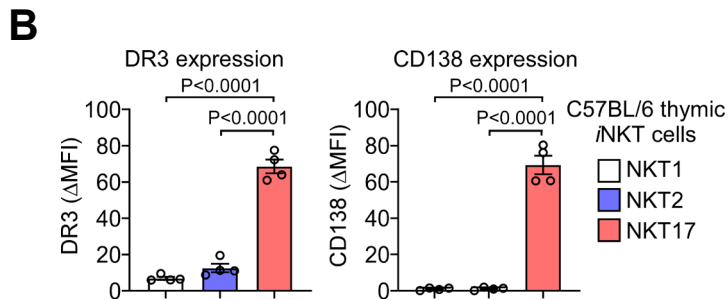
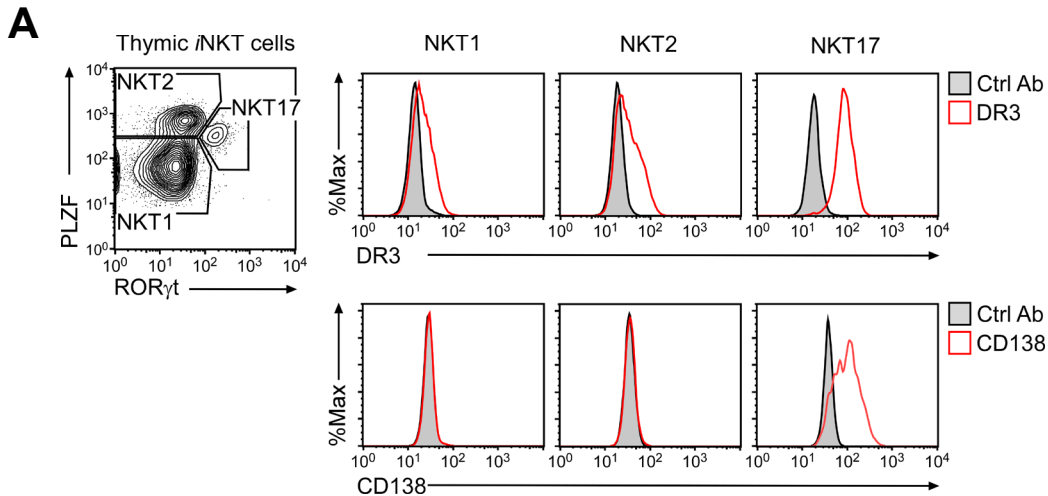


Figure 1–figure supplement 1. DR3 expression on thymic NKT17 cells of C57BL/6 mice

A. *i*NKT subsets were identified among thymocytes of C57BL/6 mice by intracellular staining for ROR γ t and PLZF and assessed for subset-specific expression of DR3 and CD138. The data are representative of 3 independent experiments.

B. Bar graphs show DR3 expression (Δ MFI) (left) and CD138 expression (Δ MFI) (right) among thymic subsets of C57BL/6 mice as identified by intracellular staining for ROR γ t and PLZF. The data are from 3 independent experiments with a total of 4 pooled C57BL/6 mice and presented as mean \pm SEM. Statistical significance was determined by unpaired two-tailed Student's *t*-tests.

Figure 1–figure supplement 2

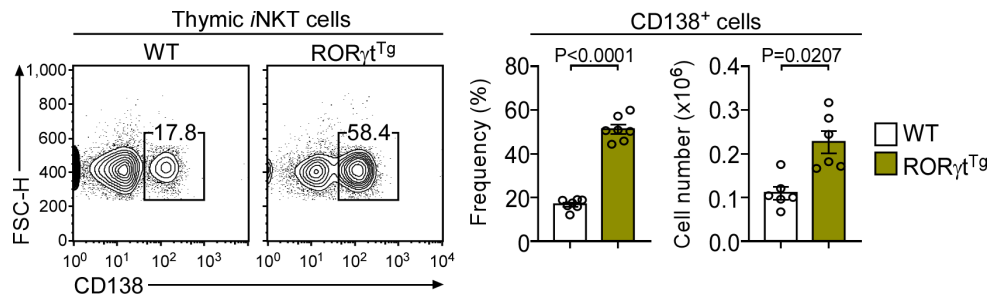


Figure 1–figure supplement 2. Thymic CD138⁺ *i*NKT cells in WT and ROR γ t^{Tg} BALB/c mice
Contour plots show CD138 versus FSC-H of *i*NKT cells in littermate control (WT) BALB/c and ROR γ t^{Tg} BALB/c mice (left). Bar graphs show the frequency and cell number of CD138⁺ *i*NKT cells in WT BALB/c and ROR γ t^{Tg} BALB/c mice (right). Contour plots are representative and bar graphs show the summary of 3 independent experiments with a total of 6 WT and 6 ROR γ t^{Tg} BALB/c mice. Data are presented as mean \pm SEM. Statistical significance was determined by paired two-tailed Student's *t*-tests.

Figure 3—figure supplement 1

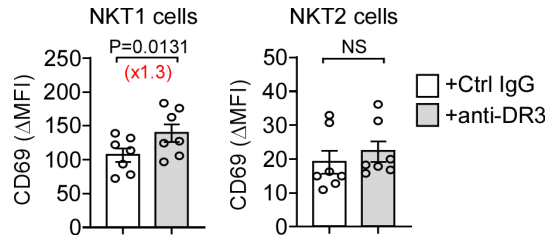


Figure 3—figure supplement 1. CD69 expression upon DR3 injection in thymic NKT1 and NKT2 cells

Bar graphs show the CD69 expression (Δ MFI) of thymic NKT1 (left) and NKT2 (right) cells in Foxp3-DTR/EGFP BALB/c mice, one week after injection with anti-DR3 or isotype control antibodies. The results are summary of 7 independent experiments with a total of 14 mice injected with either anti-DR3 antibodies (7 mice) or with isotype control antibodies (7 mice). Data are presented as mean \pm SEM. NS, non-significant. Statistical significance was determined by paired two-tailed Student's *t*-tests.

Figure 3—figure supplement 2

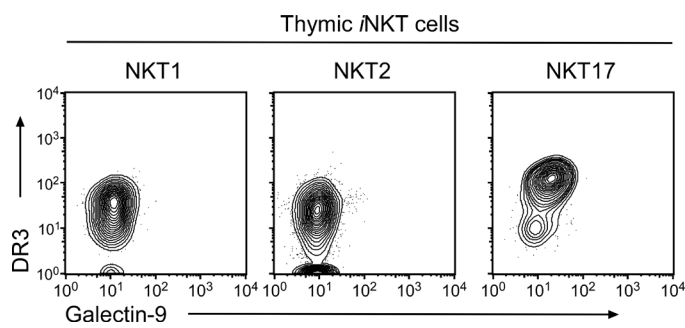


Figure 3—figure supplement 2. Galectin-9 and DR3 expression in thymic *i*NKT cell subsets of BALB/c mice

The counter plots show galectin-9 versus DR3 profiles of thymic NKT1 cells (CD122⁺), NKT2 cells (CD122⁻CD4⁺) and NKT17 cells (CD122⁻CD4⁻). The data are representative of 2 independent experiments with a total of 5 WT BALB/c mice.

Figure 3—figure supplement 3

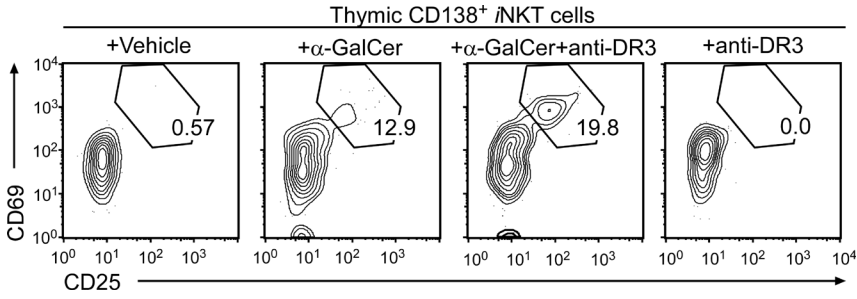


Figure 3—figure supplement 3. *In vitro* stimulation of thymic iNKT cells with α-GalCer and/or anti-DR3 antibodies

Contour plots show CD69 versus CD25 profiles of CD138⁺ thymic iNKT cells of BALB/c mice that were cultured O/N with α-GalCer and/or anti-DR3 antibodies. The data are representative of 4 independent experiments with a total of 10 WT BALB/c mice for each group.